Numerical modeling and seismic evaluation of masonry-infilled reinforced concrete frames retrofitted with carbon fiber–reinforced polymer wraps

Xiaolan Pan[1,2,3], Jiachuan Yan[1,2,3], Zhenyu Wang[1,2,3] and Chaoying Zou[1,2,3]

Abstract

This article investigates the efficiency of various retrofitting schemes using carbon fiber–reinforced polymers in improving the seismic performance of a substandard masonry-infilled reinforced concrete frame. One virtual five-story reinforced concrete frame was designed according to out-of-date Chinese codes. In total, 15 carbon fiber–reinforced polymers retrofitting schemes were adopted before earthquakes, and three sets of earthquakes representing low, medium, and high frequency contents were selected to conduct the incremental dynamic analysis. The influence of infills' collapse due to out-of-plane effect was discussed detailedly, and then, the effectiveness of different retrofitting schemes was evaluated. It was found that the collapse of infills obviously reduced the seismic capacity and finally resulted in a soft-story failure mechanism for the reinforced concrete frame. For earthquakes with low frequency content, the enhancement efficiency of retrofitting infills or both columns and infills was increased with the increase in the number of retrofitted stories; however, for medium and high earthquake frequency contents, retrofitting infills or both columns and infills were inefficient when less than half of the structure height was retrofitted. Among the adopted 15 schemes, carbon fiber–reinforced polymers retrofit of both columns and infills along the full building height was found to be the most efficient. Improper selection of a retrofitting scheme could lead to the change of soft-story location. The inter-story drift ratio capacity of effectively retrofitted frames can meet the requirements of current seismic code.

Introduction

The masonry infills are frequently used as interior partitions and exterior walls in buildings. They are usually considered as non-structural elements, and the interaction with the bounding frame is often ignored in design or seismic performance evaluation of reinforced concrete (RC) frame structures. Such an assumption is not always a conservative approach although the presence of masonry infills can increase the initial global stiffness and lateral load-carrying capacity of RC frames. It is due to the fact that the stiffer the building is, usually, the higher seismic lateral loads it attracts.

Extensive collapses of masonry-infilled RC frames in the past earthquakes (e.g. San Fernando 1971, Northridge 1994, Kobe 1995, Jabalpur 1997, Wenchuan 2008, L'Aquila 2009, Port-au-Prince 2010, Lorca 2011)

have revealed that the masonry infills have a negative influence on the seismic performance of infilled frames, such as the soft-story failure mechanism caused by vertical discontinuity of masonry infills (Dolsek and Fajfar, 2001; Verderame et al., 2011), torsional failures induced

[1]Key Lab of Structures Dynamic Behavior and Control of the Ministry of Education, Harbin Institute of Technology, Harbin, China
[2]Key Lab of Smart Prevention and Mitigation of Civil Engineering Disasters of the Ministry of Industry and Information Technology, Harbin Institute of Technology, Harbin, China
[3]School of Civil Engineering, Harbin Institute of Technology, Harbin, China

Corresponding author:
Zhenyu Wang, School of Civil Engineering, Harbin Institute of Technology, Harbin 150090, China.
Email: zhenyuwang@hit.edu.cn

by the asymmetry of infills in the plan (Correnza et al., 1994; De Stefano et al., 1998), and short-column effects due to the openings in infill walls (Bikce, 2011; Cagatay et al., 2010). Even for the RC frames with regularity in plan and elevation, the collapse of masonry walls may also lead to vertical or plan irregularity and further result in the unexpected soft-story or torsional failure mechanisms for the whole structure during earthquakes. In recent years, although numerous studies have been conducted to investigate the effect of masonry infills as structural elements on the overall seismic responses of RC frames, most of these investigations concentrated on the new buildings. However, a large number of existing masonry-infilled RC frames, which were designed and built according to out-of-date codes, are still in service in potential earthquake regions across the world. These RC frames are commonly referred to as substandard or non-ductile frames (Baran and Tankut, 2011; Ozcelik et al., 2011; Wang et al., 2016; Zou et al., 2007). The masonry infills of these frames are generally poorly connected to the bounding frames and thus face at high risk of collapse under the future strong earthquakes. Following major earthquake events, unsatisfactory performance (i.e. collapse) of masonry infills in these frames has been repeatedly reported (Braga et al., 2011). To improve the seismic safety of RC structures, there is an urgent need for the seismic retrofit of existing substandard infilled RC frames before earthquakes, which has become a key issue for the engineers around the world.

Externally bonded fiber-reinforced polymer (FRP) composites, as a relatively new strengthening technique, have been widely used for seismic retrofitting of RC structures in the past two decades, due to their high strength, light weight, ease of application, and minimum disturbance to the occupants. Although many experimental and analytical investigations have been conducted by researchers all over the world, most of them have been concentrated on the member-level behavior (Al-Salloum and Almusallam, 2007; Carpinteri et al., 2009; Dandapat et al., 2011; Deng et al., 2015; Mukherjee and Jain, 2013; Smith and Teng, 2002; Wang et al., 2013). The studies on the structure-level behavior of FRP-retrofitted RC frames were relatively limited and mostly focused on the FRP retrofit of bare frames without including the effects of masonry infills (Galal and El-Sokkary, 2008; Garcia et al., 2010; Ma et al., 2013; Wang et al., 2016). These limited studies have confirmed the efficiency of externally bonded FRP in improving the structural seismic performance of bare RC frames.

Researches on seismic evaluation of FRP-retrofitted masonry-infilled RC frames received greater attention after the last decade. However, the research efforts were largely limited to the basic one-story one-bay structures retrofitted with FRP (Altın et al., 2008,

2012; Kakaletsis, 2011; Ozkaynak et al., 2011; Yuksel et al., 2010). These experimental studies indicated that the reasonable FRP retrofitting schemes could significantly enhance the overall structural seismic performance by preventing the brittle failure and out-of-plane instability of infill walls, changing the load transfer path between infills and RC frame, reducing the damage to the joint core regions, and improving the seismic resistance of beams and columns. Also, other few studies have been conducted on the seismic investigation of FRP-retrofitted multi-story infilled RC frames (Akin et al., 2014; Binici et al., 2007; El-Sokkary and Galal, 2009; Erdem and Akyuz, 2010). Although the above studies validated the feasibility and efficiency of FRP retrofitting of infilled RC frames, these investigations mainly concentrated on one- or two-story frames, and the variety of retrofit techniques was rather limited. Further studies are therefore necessary to qualitatively and quantitatively evaluate the effectiveness of various FRP retrofit schemes for upgrading the overall seismic performance of multi-story infilled RC frames.

Against this background, this article presents an analytical evaluation on the seismic enhancement efficiency of various FRP retrofitting schemes applied for a typical substandard low-rise RC frame with masonry infills. One five-story masonry-infilled RC frame was designed according to out-of-date Chinese codes (Ministry of Construction of the People's Republic of China, GB50010, 2002). A total of 15 different FRP retrofitting schemes were adopted before earthquake excitations for the substandard frame. Three sets of ground motion records, representing low, medium and high acceleration-to-velocity (A/V) ratios, respectively, were selected to conduct the incremental dynamic analysis (IDA). The influence of collapse of infills due to out-of-plane effect on the overall seismic behaviors of the designed frame was first investigated in terms of maximum peak ground acceleration (PGA), maximum inter-story drift ratio (IDR), and failure mechanisms. Then, the seismic responses of the infilled frame before and after retrofitted with various schemes were compared in regard to the maximum PGA, maximum IDR, and energy dissipation capacities. The effective retrofitting schemes using carbon fiber–reinforced polymers (CFRP) for the substandard low-rise masonry-infilled RC frame were recommended based on the analysis results.

Details of the selected RC frame

To represent existing substandard low-rise frames, one typical five-story masonry-infilled RC frame was designed for gravity loads only according to the old national design code of concrete structures in China
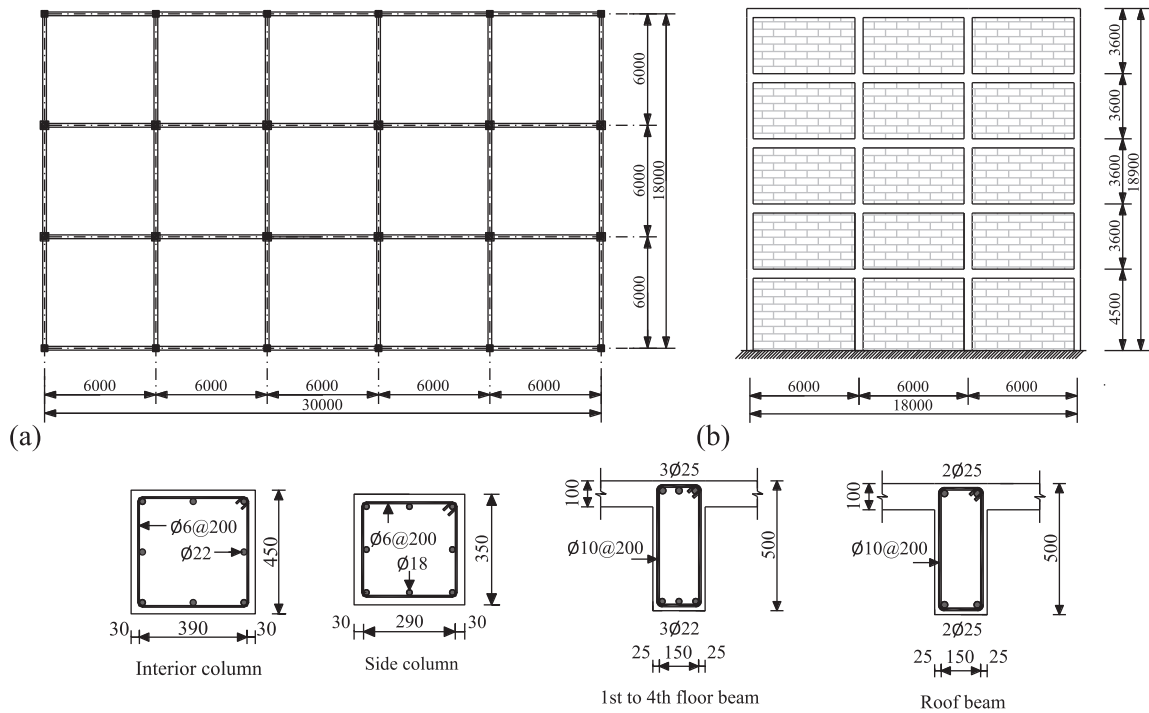
Figure 1. (a) Plan and (b) elevation of the studied building (units: mm).

(Ministry of Construction of the People's Republic of China, GB50010, 2002). The plan and elevation of the frame as well as the steel reinforcements are shown in Figure 1. The interior and side columns had a longitudinal reinforcement ratio of 1.5% and 1.66%, respectively. The floor and roof slabs were assumed to carry a uniform dead load of 5 and 6 kN/m^2, respectively, plus a live load of 2 kN/m^2. The weights of masonry walls were treated as uniform loads acting on the beams. The compressive strength of concrete was 25 MPa, and the yield strengths of longitudinal reinforcements and lateral hoops were 360 and 260 MPa, respectively. The modulus of elasticity of concrete and steel bars was 20 and 200 GPa, respectively. The thickness of concrete cover for slabs, beams, and columns was 15, 25, and 30 mm, respectively. The masonry infills with a thickness of 120 mm were constructed with solid clay bricks that were commonly used in existing frames across China. The masonry unit and mortar had a compressive strength of 10 and 5 MPa, respectively. The elastic modulus of the infill wall was taken as 2.8 GPa. The axial compression ratios for the interior and side columns at the ground floor were approximately identical, with the values equal to 0.35 and 0.34, respectively.

Selection of ground motion records

In seismic analyses, the seismic behavior of structures is closely related to the dynamic properties of input ground motions. Tso et al. (1992) investigated the significance of the peak ground acceleration-to-velocity (A/V) ratio as a parameter to indicate the dynamic characteristics of earthquake ground motions and found that the A/V ratio can be used as a simple parameter to indicate the frequency content of the ground motion. On the basis of this result, nine actual ground acceleration records were obtained from the Pacific Earthquake Engineering Research (PEER) Center strong motion database for the IDA analysis. These records were divided into three sets representing low (A/V < 0.8 g s/m), medium (0.8 g s/m ⩽ A/V ⩽ 1.2 g s/m), and high (A/V > 1.2 g s/m) frequency contents, respectively. This is useful to evaluate the effect of earthquake frequency content on the seismic behavior of the studied frames. The details of selected ground motions are summarized in Table 1.

Retrofitting schemes

To find the effective CFRP retrofitting techniques for the selected substandard frame, 15 retrofit schemes were considered in this study. The detailed information of the 15 retrofitting schemes is presented in Table 2. From the experimental testing and analytical results (Wang et al., 2012c), it was found that the ductility capacity of columns wrapped with four layers of CFRP sheets was improved significantly and could

Table 1. Details of the selected ground motion records.

No.	Ground motion	Station	Component	Date	Magnitude (Ms)	PGA (g)	PGV (m/s)	A/V (g s/m)	Levels
1	Chi-Chi	ALS	E	20 September 1999	7.6	0.183	0.393	0.466	Low
2	Loma Prieta	1028 Hollister City Hall	090	18 October 1989	7.1	0.247	0.385	0.642	Low
3	Düzce	Düzce	270	12 November 1999	7.3	0.535	0.835	0.641	Low
4	Northridge	24278 Castaic-Old Ridge Route	090	17 January 1994	6.7	0.568	0.521	1.090	Medium
5	Kobe	0 KJMA	000	16 January 1995	–	0.821	0.813	1.010	Medium
6	Imperial Valley	117 El Centro Array #9	180	19 May 1940	7.2	0.313	0.298	1.050	Medium
7	Loma Prieta	57425 Gilroy Array #7	090	18 October 1989	7.1	0.323	0.166	1.946	High
8	Whittier Narrows	24461 Alhambra, Fremont Sch	270	01 October 1987	5.7	0.414	0.163	2.540	High
9	San Fernando	128 Lake Hughes #12	021	09 February 1971	6.6	0.366	0.170	2.153	High

PGA: peak ground acceleration; PGV: peak ground velocity.

Table 2. Detailed information of retrofitting schemes.

Type of retrofitted elements	Location of retrofitted elements				
	First story	First to second story	First to third story	First to fourth story	First to fifth story
Columns only (i.e. Figure 2(a) and (b))	scheme 1	scheme 2	scheme 3	scheme 4	scheme 5
Infills only (i.e. Figure 2(c))	scheme 6	scheme 7	scheme 8	scheme 9	scheme 10
Columns and infills	scheme 11	scheme 12	scheme 13	scheme 14	scheme 15

reach up to 2.5 times that of non-retrofitted ones. Hence, for the retrofit of columns in this study, four CFRP layers with a height of 1.5hc (hc is the height of column section) were wrapped in the lateral direction at the potential plastic hinge regions (i.e. at both ends of columns), as shown in Figure 2(a) and (b). The corner radius was set as a constant value of $0.15h_c$ on account of the position of the internal steel reinforcement. For masonry infills, the seismic retrofit should consider the most stressed part of the infill and the possible detachment regions under a lateral load. It is evident from the available literature that the stressed part of the infill is a diagonal region connecting the two loaded corners. Based on this, one layer of X-shaped CFRP sheets was diagonally applied on both sides of the infill wall, which can be seen in Figure 2(c). X-shaped CFRP strips were used to resist tension stress only under the cyclic earthquake loads. The properties of utilized unidirectional CFRPs were ultimate tensile strength f_{CFRP} = 4340 MPa, modulus of elasticity E_{CFRP} = 244 GPa, and layer thickness of 0.167 mm.

Numerical modeling

In this study, the PERFORM-3D software was utilized for the numerical modeling and nonlinear analyses of the RC frames. Due to the plan symmetry of the analyzed building, three-span five-story two-dimensional (2D) models were built for the frames before and after retrofitting. Second-order (P–Δ) effects were included in the analysis. The case of retrofitting first floor columns and infills (i.e. scheme 11) is selected to illustrate the numerical modeling method adopted in this study, as shown in Figure 3.

Beams and columns

The beams and columns were modeled using nonlinear beam–column elements with distributed plasticity. The cross sections of the beams and columns were discretized into a number of fibers with appropriate uniaxial stress–strain responses for different materials (i.e. concrete, steel bars). The mesh size for discrete fibers was determined when the load–displacement curve
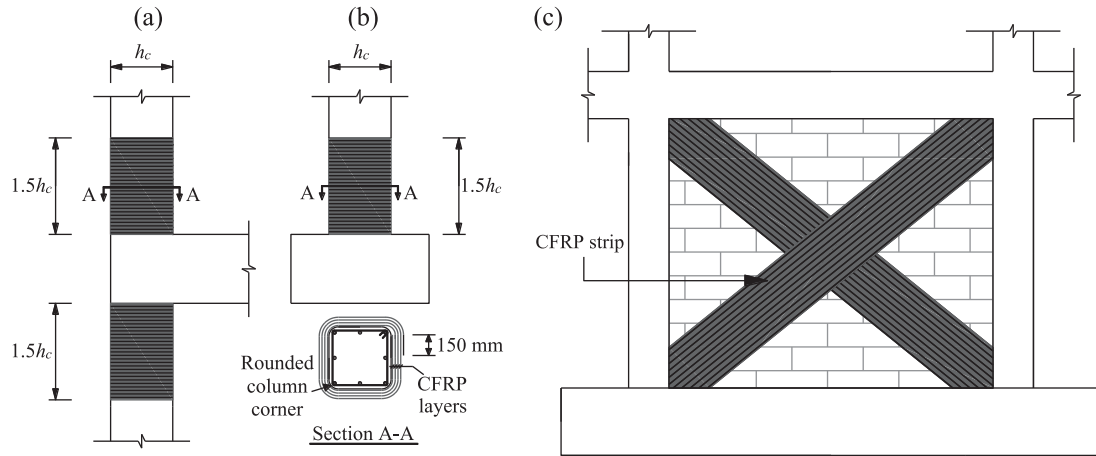
Figure 2. CFRP strip configuration used for: (a) column ends, (b) bottom of first story columns, and (c) masonry infills.
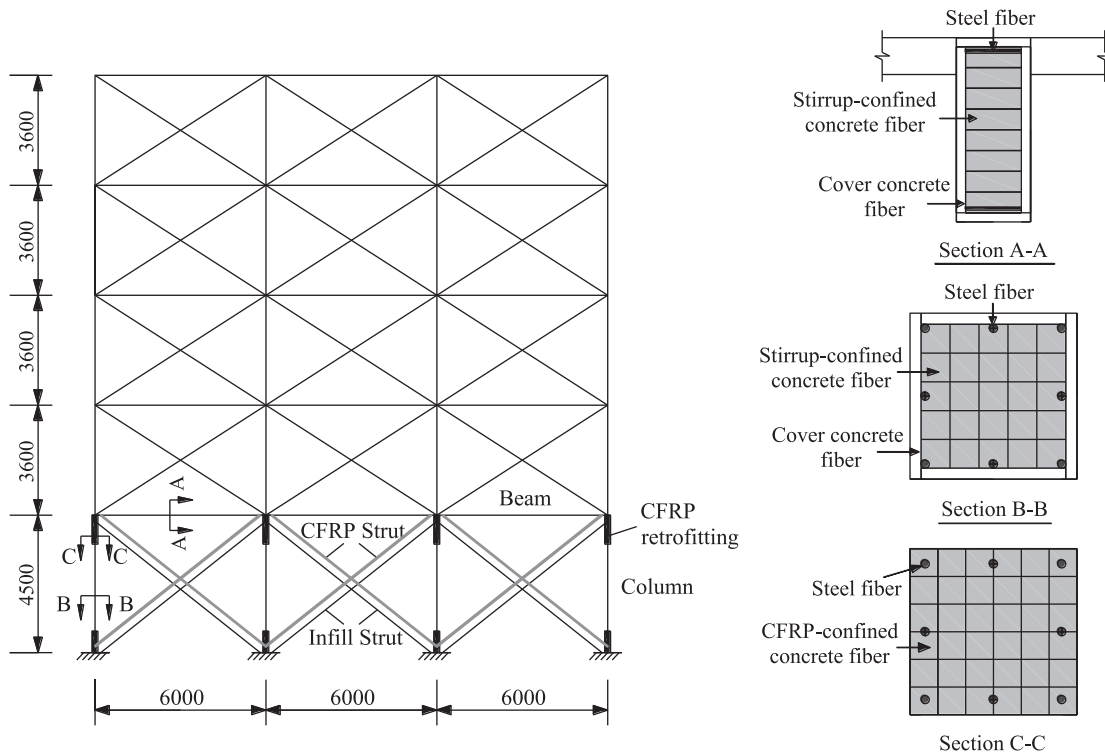

Figure 3. Finite element model for retrofitting scheme 11 (dimensions in mm).

obtained from the pushover analysis did not differ by more than 5% from that obtained from the model with a mesh size twice as large as the one used.

In PERFORM-3D, a multi-linear backbone curve is used to define the compressive stress–strain relationship of the concrete as shown in Figure 4(a). The stress and strain at the characteristic points (i.e. the Y, U, L, R, and X points) need to be determined. For cover concrete and stirrup-confined core concrete fibers, the uniaxial stress–strain model proposed by Guo (1999)

was adopted to calculate the stress and strain values at characteristic points. For CFRP-confined concrete fibers, the axial compressive stress–strain model proposed by Wang et al. (2012a, 2012b) was selected to calculate the characteristic values. The hysteretic behavior of the adopted multi-linear model is defined by the use of the energy degradation factor (EDF) that represents the ratio between the area of degraded hysteresis loop $S_{degraded}$ and the area of non-degraded loop $S_{non-degraded}$ (PERFORM-3D User Guide, 2011)
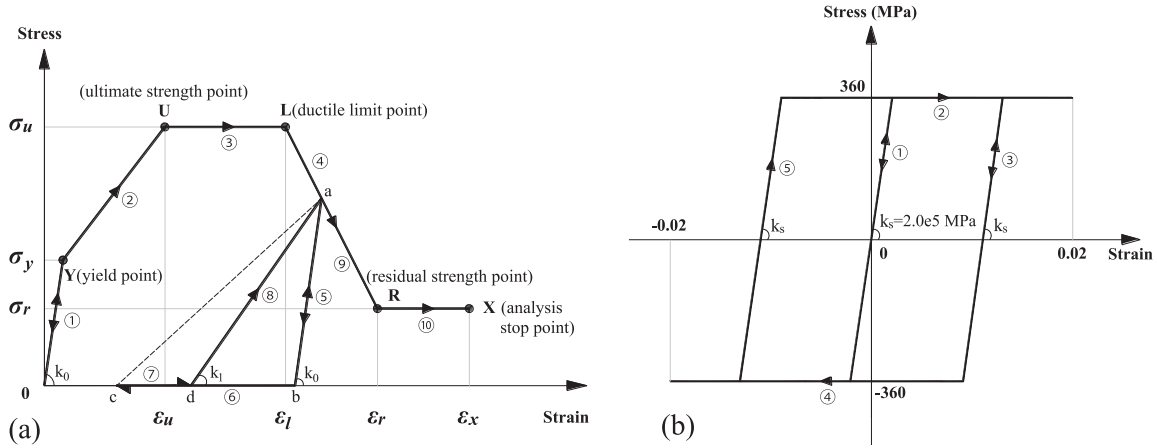
Figure 4. Cyclic stress–strain relationship of: (a) concrete and (b) steel bars.

Table 3. The parameters used for the concrete model (unit of σ: MPa).

Characteristic points	Parameters	Cover	Stirrup-confined		CFRP-confined		EDF
			Beam	Column	Side column	Interior column	
Point Y	σ_y	14.0	22.0	18.0	21.8	20.0	1.0
	ε_y	0.0007	0.0011	0.0009	0.0011	0.0010	
Point U	σ_u	25.0	26.0	25.2	38.1	35.8	0.9
	ε_u	0.0017	0.0023	0.0015	0.0040	0.0035	
Point L	σ_l	25.0	26.0	25.2	38.1	35.8	0.7
	ε_l	0.0023	0.0025	0.0027	0.0060	0.0060	
Point R	σ_r	1.0	2.6	8.1	36.7	31.3	0.4
	ε_r	0.0100	0.0170	0.0085	0.0122	0.0110	
Point X	σ_x	1.0	2.6	8.1	36.7	31.3	0.3
	ε_x	2.0000	0.0600	0.0500	0.0332	0.0267	

$$\text{EDF} = \frac{S_{degraded}}{S_{non-degraded}} = \frac{S_{\Delta abd}}{S_{\Delta abc}} \qquad (1)$$

where $S_{\Delta abd}$ and $S_{\Delta abc}$ represent the area of degraded and non-degraded loop, respectively. It also assumes that there is no stiffness degradation during unloading process, and the EDFs between adjacent characteristic points follow a linear change. The parameters used for the concrete model are listed in Table 3.

For the steel reinforcement, a typical elastic–plastic model without stiffness degradation and strength loss was used, as shown in Figure 4(b). In this model, the EDF was always assumed to be 1.0. In the following analysis, this assumption was proved to be reasonable based on the fact that no local failure had happened before reaching the drift limit for the studied frames by tracking the strain history in the steel fibers.

Masonry infill walls

As the objective of this study was to investigate the effect of CFRP retrofitting on the global behavior of the RC frames, the single diagonal strut model was used in absence of more refined models as shown in Figure 5(a). Under the repeated seismic loading, X-shaped diagonal struts were placed between the beam–column connections to provide a lateral load resisting mechanism for the opposite lateral directions. The diagonal struts were assumed to resist axial compressive stress only since the tensile strength of masonry was negligible. The cross-sectional area of each strut was calculated as the product of the infill thickness and the equivalent strut width. The width of the equivalent diagonal strut was determined through equation (2) proposed by Masonry Standards Joint Committee (MSJC) which was a modified version of Bennett et al.'s (1996) equation

$$w = \frac{0.3}{\lambda \cos \theta} \qquad (2)$$

$$\lambda = \sqrt[4]{\frac{E_m t_m \sin 2\theta}{4 E_c I_c h_m}} \qquad (3)$$

where w is the width of the equivalent strut; λ is the characteristic stiffness parameter; E_m is the elastic
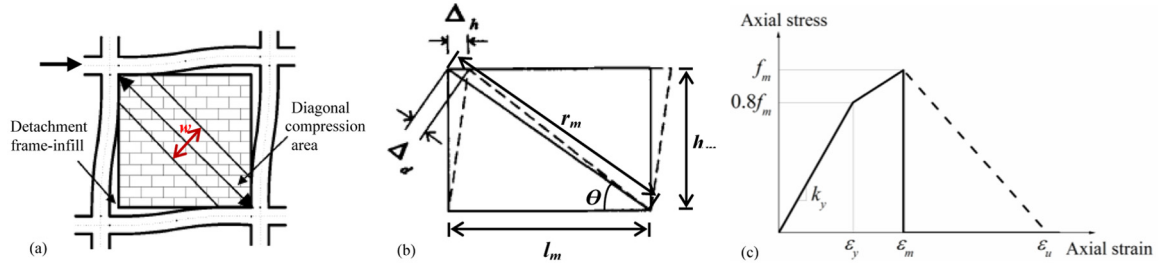
Figure 5. (a) Strut model analogy of the infill, (b) deformation, and (c) axial stress–axial strain relationship of the infill compression strut.

modulus of the infills; h_m and t_m are the height and thickness of the infills, respectively; E_c and I_c are the elastic modulus and moment of inertia of the frame columns, respectively; θ is the inclination of the infill diagonal ($\tan\theta = h_m/l_m$); and l_m represents the length of the masonry walls.

Although the sudden collapse of masonry infills in RC frames due to out-of-plane earthquake excitation has been repeatedly reported following major earthquake events, few investigations took into account its effect on the seismic performance of masonry-infilled RC frames. At present, most studies adopted a multi-linear model with a descending branch over the peak strength for the infill compression strut, as shown by the dashed line in Figure 5(c). However, this common practice fails to consider the effect of the abrupt collapse of infills resulting from the out-of-plane excitation while the out-of-plane earthquake may result in total collapse of the infill when it enters the instability stage (i.e. the descending branch), as is indicated by the study conducted by Hashemi and Mosalam (2008). This is especially true for existing substandard frames whose infills are usually poor or have no connections with the bounding frames. Hence, in this study, a model with the peak strength followed by a sudden loss of the lateral strength was assumed for the equivalent strut, as shown by the solid line in Figure 5(c). The maximum axial strength f_m of the strut equaled 3.33 MPa in this study. The initial stiffness k_y was calculated as four times the secant stiffness at the peak strength (Uva et al., 2012). The axial strain ε can be calculated as follows

$$\varepsilon = \frac{\Delta_d}{r_m} = \frac{\Delta_h \cos\theta}{r_m} = \frac{Dh_m l_m}{r_m^2} \quad (4)$$

where r_m is the diagonal length of infill wall; Δ_d and Δ_h represent the infill diagonal and horizontal deformation, respectively, as is shown in Figure 5(b); and D denotes the IDR and is chosen as 0.1% and 0.6% for ε_m and ε_u, respectively, according to FEMA-356 (2000a).

X-shaped CFRP strips

Because the CFRP strips can only sustain tension, so uniaxial tension struts were used to model the X-shaped CFRP strips applied on both sides of the masonry infills. In this study, the CFRP strips were modeled as linear elastic material with maximum axial strain of 0.003 and corresponding maximum axial stress of 732 MPa. These values took into account the characteristics of CFRP, plaster, infill, as well as the effect of FRP delamination and failure of anchorages. The cross-sectional area of each tension strut was calculated as the product of the total thickness of CFRP strips adopted on both sides of infills and the width of CFRP sheets that was identical with the equivalent width of masonry compression struts. Similar modeling approach for the X-shaped CFRP strips was also used in the analytical study conducted by other researchers (Binici et al., 2007; El-Sokkary and Galal, 2009).

Verification of the numerical model

To verify the accuracy of the nonlinear analysis results, the shake table test conducted by Hashemi and Mosalam (2006) at the Richmond Field Station of the University of California, Berkeley, was simulated in this study. A one-story one-bay by two-bay RC frame containing unreinforced masonry (URM) wall was tested in three distinct stages. The selected ground motions were scaled to generate different levels of intensity and were applied as unidirectional motions in the direction parallel to the URM infill wall. The specimen subjected to the Northridge record with low-intensity levels (i.e. TAR1, TAR2, and TAR3) in stage 1 was analyzed using PERFORM-3D. This was for two reasons: (1) the infill wall was destroyed and removed after the first stage of test and (2) the accumulated damage in the structure was insignificant under low-intensity earthquake excitations and thus the influence of loading history can be ignored. Figure 6 compares the acceleration time history responses at the top of the structure. It can be seen
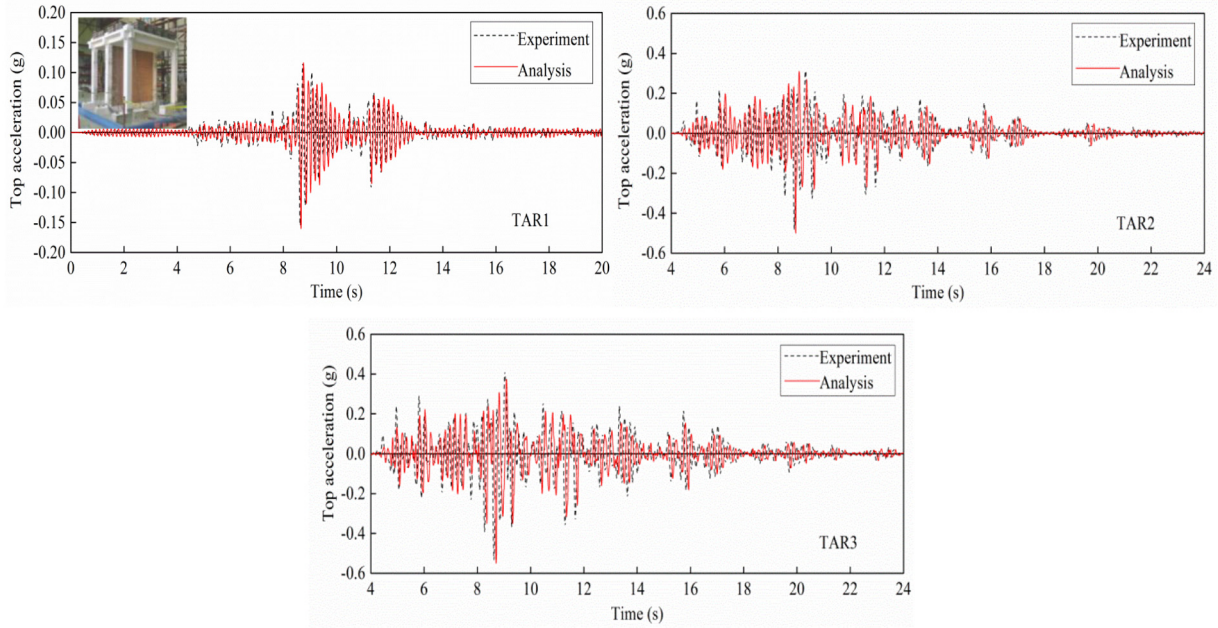
Figure 6. Comparison of top acceleration time histories between the experimental and analytical results.
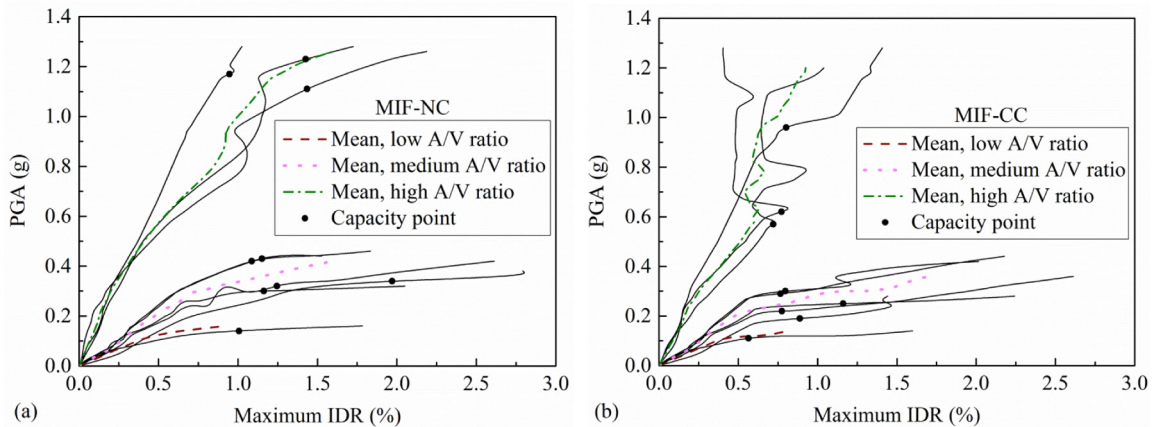

Figure 7. IDA curves for (a) MIF-NC and (b) MIF-CC frames.

that the analytical and experimental results are in good agreement for the three studied cases. In addition, the fundamental period of the analytical model was calculated to be 0.1388 s which differed only by 5.58% from the experimental value of 0.147 s. These results indicated that the employed numerical model could sufficiently simulate the nonlinear dynamic behavior of the test specimen.

Analysis results and discussion

The IDA analyses were conducted for the designed frame before and after CFRP retrofitting. According

to Vamvatsikos and Cornell (2002), the IDA analysis is a parametric analysis method to estimate more thoroughly structural performance under seismic loads. An IDA curve is a plot of a state variable (i.e. damage measure, DM) recorded in an IDA study versus one or more intensity measures (IMs) that characterize the applied scaled accelerogram. The PGA has long been used as an IM to characterize the "intensity" of a ground motion record. For structural damage of frame buildings, the IDR relates well to joint rotations and both global and local story collapse, thus becoming a strong DM candidate. Therefore, the PGA and IDR were chosen as the IM and DM, respectively, to
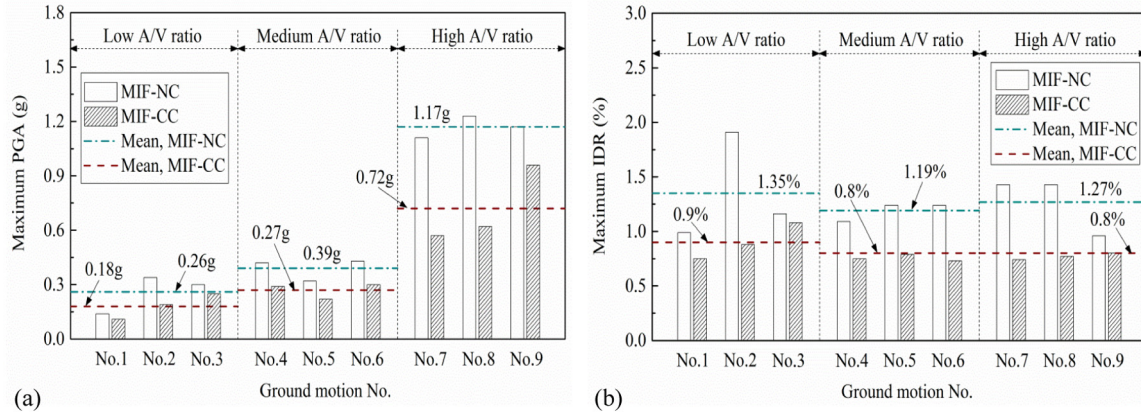
Figure 8. (a) Maximum PGA and (b) maximum IDR capacities for MIF-NC and MIF-CC frames.

produce the IDA curves in this study. The PGA of the selected ground motions was scaled according to an increment of 0.05 g.

Influence of collapse of infills due to out-of-plane effect

In the following analysis, the masonry-infilled frame considering and neglecting the collapse of infills due to out-of-plane effect was denoted as MIF-CC and MIF-NC, respectively. Both of them were substandard frames without CFRP retrofitting. For this part, their seismic responses were compared with respect to maximum PGA and IDR capacities as well as failure mechanisms.

Figure 7 shows the IDA curves for MIF-NC and MIF-CC frames. It can be seen that the maximum IDR responses of both frames decreased with the increase in A/V ratio of the selected ground motions at the same PGA level, which was indicated by the leftward shift of the IDA curves for earthquakes with higher frequency contents. This means that the frames exhibit larger displacement responses under lower A/V ratio earthquakes. Based on the IDA curves, the maximum PGA resisted by the frames was obtained using the FEMA (2000b) 20% tangent slope approach. In this approach, the point on the IDA curve with a tangent slope equal to 20% of the elastic slope is defined to be the capacity point. Figure 8(a) shows the maximum PGA resisted by MIF-NC and MIF-CC frames. It can be seen that the maximum PGA resisted by MIF-CC decreased significantly due to the collapse of infills, especially for earthquakes with high A/V ratio. For example, the maximum PGA capacity of MIF-CC (0.62 g) reduced by almost 50% under the Whittier Narrows record (ground motion no. 8) compared to that of MIF-NC (1.23 g). The mean maximum PGA of MIF-CC decreased by 30.8%, 30.8%, and 38.5%,

respectively, for low, medium, and high A/V ratio earthquakes. In addition, it was also noted that the PGA capacity was significantly dependent on the frequency content of the ground motion. The mean values of maximum PGA resisted by both frames increased rapidly with the increase in A/V ratio of the earthquake records. This is consistent with the results obtained from Figure 7 that the frames tend to have larger displacement responses under earthquakes with lower A/V ratios.

Besides the maximum PGA, the maximum IDR capacity for MIF-NC and MIF-CC frames was also compared, as shown in Figure 8(b). The IDR was calculated at each floor by dividing the difference in the lateral displacement of two successive floors over the story height. The maximum IDR capacity was defined as the maximum IDR calculated when the frame was subjected to the maximum PGA that can be resisted. From Figure 8(b), the collapse of infills resulted in an obvious reduction in the maximum IDR capacity of RC frames. The most significant decrease of 54% was observed for Loma Prieta record (ground motion no. 2), reducing from 1.91% for MIF-NC to 0.88% for MIF-CC. The mean maximum IDR capacities for earthquakes with low, medium, and high frequency contents were reduced by 33.3%, 32.8%, and 37.0%, respectively. This was similar to the results for maximum PGA capacity as discussed above. However, it was worth noting that the earthquake frequency content (A/V ratio) had a very slight influence on the IDR capacity of RC frames. This justifies the validity and rationality of using the maximum IDR as a uniform and reliable damage parameter to judge the performance of structures.

The remarkable decrease in maximum PGA and IDR capacities of MIF-CC frame can be attributed to the change of structural failure mechanism resulting from the collapse of infills. Take the case of Düzce

record (ground motion no. 3) for an example; the formation of plastic hinges in beams and columns is presented in Figure 9 when the maximum PGA level is applied for both frames. It can be seen that the plastic hinges were first developed in beams for MIF-NC frame. By contrast, the plastic hinges occurred in columns first and only for MIF-CC frame. The reason was that the first story became obviously weaker than the upper stories after the masonry infills at the ground floor collapsed, which finally resulted in a soft-first-story failure mechanism for the MIF-CC structure.

The above observations indicated that the sudden collapse of masonry infills due to out-of-plane effect could have an adverse impact on the overall seismic performance of infilled RC frames. The effective retrofitting techniques are thus needed for existing substandard RC frames with masonry infills that are at high risk of collapse during possible strong earthquakes in the future.

Evaluation of different retrofitting schemes

In this section, 15 different retrofitting schemes were evaluated for the substandard infilled frame considering the out-of-plane effect on collapse of infills (i.e. MIF-CC). The frame without retrofitting (i.e. MIF-CC) was used as the control frame. The seismic behaviors between the control and retrofitted frames were compared in terms of maximum PGA, IDR, and energy dissipation capacities.
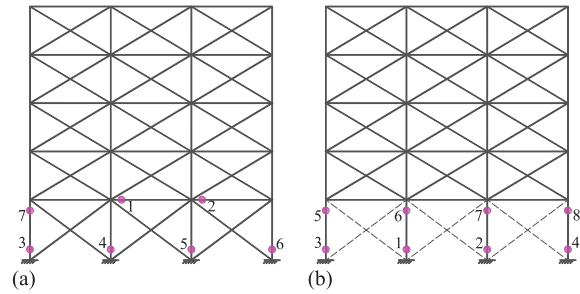

Figure 9. Formation of the plastic hinges for: (a) MIF-NC and (b) MIF-CC frames (circular dots indicate beam and column hinges; numbers represent the sequence of occurrence of the plastic hinges; and diagonal dotted lines indicate collapse of infills).

Figure 10 presents the mean IDA curves of the control and retrofitted frames. Based on the IDA analysis results, the maximum PGA resisted by control and retrofitted RC frames were obtained using the FEMA (2000b) 20% slope criterion, as shown in Table 4. It can be seen that CFRP retrofit could generally increase the maximum PGA capacity of the control frame. Moreover, the maximum PGA resisted by control and retrofitted frames increased with the increase in the A/V ratio of earthquake records.

To better compare the efficiency between various retrofitting schemes, the PGA capacity ratio, which was defined as the ratio of the maximum PGA resisted by retrofitted frame to that resisted by control frame, was calculated and shown in Figure 11. It was noted that the PGA capacity ratios of retrofit schemes 1–5

Table 4. Maximum PGA resisted by the control and retrofitted frames (units: g).

| Retrofitting scheme no.	Ground motion no.											
	Low A/V ratio				Medium A/V ratio				High A/V ratio			
	1	2	3	Mean	4	5	6	Mean	7	8	9	Mean
Control	0.11	0.19	0.25	0.18	0.29	0.22	0.30	0.27	0.57	0.62	0.96	0.72
1	0.13	0.25	0.24	0.21	0.31	0.22	0.30	0.28	0.55	0.61	1.00	0.72
2	0.13	0.46	0.24	0.28	0.30	0.24	0.31	0.28	0.55	0.61	1.00	0.72
3	0.13	0.26	0.24	0.21	0.31	0.22	0.31	0.28	0.55	0.68	0.99	0.74
4	0.13	0.26	0.24	0.21	0.30	0.22	0.31	0.28	0.58	0.61	0.99	0.73
5	0.13	0.26	0.24	0.21	0.30	0.22	0.31	0.28	0.57	0.61	0.99	0.72
6	0.13	0.23	0.23	0.20	0.32	0.23	0.28	0.28	0.52	0.60	1.08	0.73
7	0.15	0.28	0.28	0.24	0.38	0.19	0.28	0.28	0.51	0.58	0.97	0.69
8	0.19	0.23	0.34	0.25	0.47	0.23	0.27	0.32	0.49	0.64	1.02	0.72
9	0.18	0.39	0.42	0.33	0.65	0.39	0.49	0.51	0.60	1.09	1.40	1.03
10	0.18	0.38	0.40	0.32	0.65	0.39	0.53	0.52	0.97	1.06	1.55	1.19
11	0.13	0.23	0.23	0.20	0.31	0.22	0.28	0.27	0.53	0.60	1.03	0.72
12	0.16	0.17	0.28	0.20	0.37	0.19	0.28	0.28	0.45	0.58	0.79	0.61
13	0.19	0.37	0.34	0.30	0.47	0.22	0.27	0.32	0.51	0.61	0.97	0.70
14	0.19	0.46	0.42	0.36	0.82	0.40	0.40	0.54	0.60	1.03	1.32	0.98
15	0.19	0.65	0.64	0.49	1.06	0.80	0.87	0.91	1.00	2.13	3.99	2.37

PGA: peak ground acceleration.
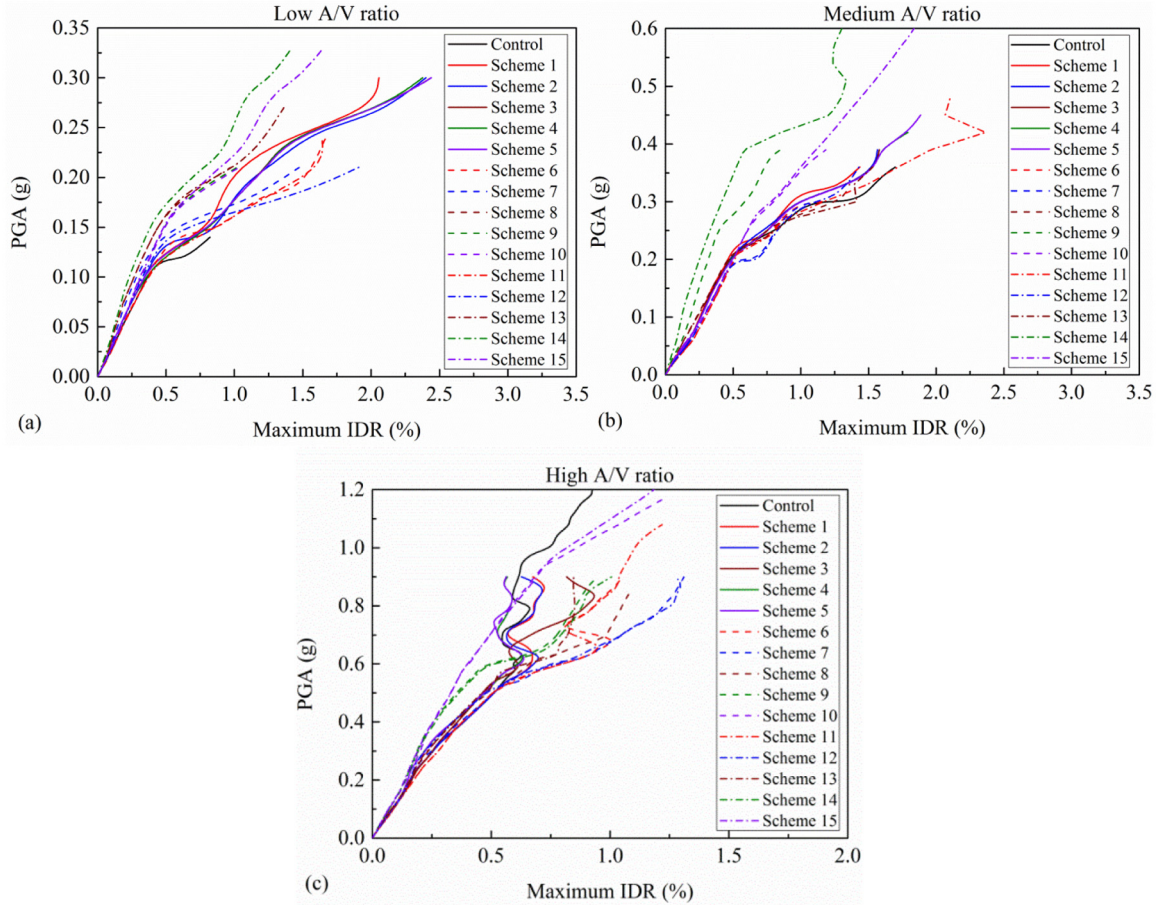
Figure 10. Mean IDA curves for the control and retrofitted frames: (a) low A/V ratio, (b) medium A/V ratio, and (c) high A/V ratio.

were basically around 1.0, especially for the medium and high A/V ratio earthquakes. It meant that CFRP retrofit of columns only at either some or all stories had little effect on improving the maximum PGA capacity of the control frame. The reason was that the structural behavior was still controlled by the nonductile infill, and the collapse of infills could not be avoided by retrofitting columns only. For the schemes of retrofitting infill walls only (i.e. schemes 6–10), the maximum PGA capacity under earthquakes with low A/V ratio (Figure 11(a)) was increased continually when CFRP retrofitting of infills extended gradually from the bottom to the top floors. However, the results for medium and high A/V ratios (see Figure 11(b) and (c)) indicated that although retrofitting the infills of bottom four or all stories (i.e. schemes 9 and 10) could significantly improve the maximum PGA capacity of the control frame, retrofitting the infills below the fourth floor (i.e. schemes 6–8) just had a very limited effect. This was because that the collapse of nonductile infills at the upper story could still result in a soft-story failure mechanism at the upper

non-retrofitted story when the lower story infills of the structure were retrofitted, as is revealed by Figure 12.

Figure 12(a) and (b) shows the plastic hinge formation for the cases of retrofitting only infills at the ground floor (i.e. scheme 6) and over the bottom three stories (i.e. scheme 8), respectively, when subjected to the maximum PGA level of Kobe earthquake (ground motion no. 5). It was noted that the collapse of infills and plastic hinges in columns occurred at the second story when the first floor infills were retrofitted with X-shaped CFRP (see Figure 12(a)), while they happened at the fourth story as a result of the CFRP retrofit of infill walls along the bottom three floors (see Figure 12(b)). Comparing Figure 12 with Figure 9(b), it was demonstrated that the location of weak story transferred from the first floor to the upper non-retrofitted floor after the control frame (i.e. MIF-CC) was enhanced with CFRP. The above conclusions for the schemes of retrofitting infills only also applied to the cases of retrofitting both columns and infills (i.e. schemes 11–15), however, the latter was more effective if the bottom four or all stories were retrofitted.
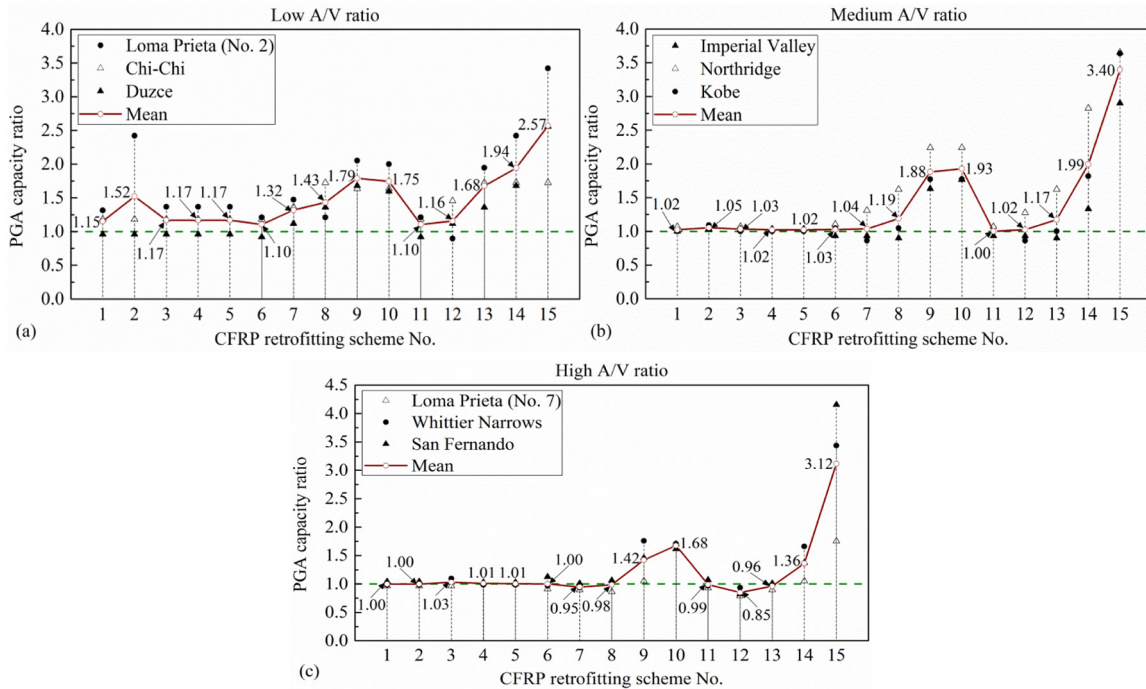
Figure 11. PGA capacity ratio of retrofitted frames: (a) low A/V ratio, (b) medium A/V ratio, and (c) high A/V ratio.

The mean values of the maximum IDR capacity for control and retrofitted frames are presented in Figure 13. It was evident that for earthquakes with different A/V ratios, retrofitting columns only had a negligible influence on the IDR capacity of the control frame. Retrofitting infills only could provide a degree of enhancement of the maximum IDR capacity under low A/V ratio records, and the increase appeared to be more significant when more floors were retrofitted (Figure 13(a)).

However, in the cases of medium and high A/V ratios, retrofitting only infills would be not effective in improving the structural IDR capacity unless the masonry infills of all stories were retrofitted (Figure 13(b) and (c)). Similar findings were also obtained for the schemes of retrofitting both columns and infills. According to the national seismic design code (Ministry of Construction of the People's Republic of China, GB50011, 2010), the capacity for the ultimate IDR is 2% for RC frames. It was worth noting in Figure 13 that the maximum IDR capacity of the control frame was less than 2%, while it reached over 2% for some retrofitted frames. This suggested that the ultimate ductility capacity of existing substandard RC frame was improved to meet the code requirements when it was effectively retrofitted with CFRP.

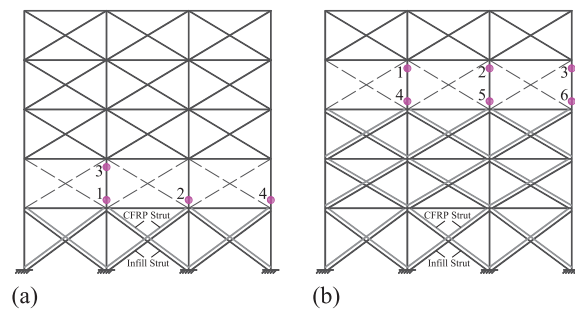Energy dissipation capacity is an important indicator of the structure's ability to withstand severe ground

Figure 12. Formation of the plastic hinges for retrofitting: (a) scheme 6 and (b) scheme 8.

motions. Figure 14 shows the mean values of maximum energy dissipated by the control and retrofitted frames. It can be seen that for three earthquake frequency contents, the maximum dissipated energy of the control frame was little improved by the use of retrofitting columns only. The cases of retrofitting only infills or retrofitting both columns and infills could effectively improve the energy dissipation capacity under low A/V ratio records, and the increase was more profound as the number of retrofitted stories increased while they were almost ineffective under medium and high A/V ratio earthquakes when some or all stories below the fourth floor were retrofitted (i.e. schemes 6–8 and schemes 11–13).
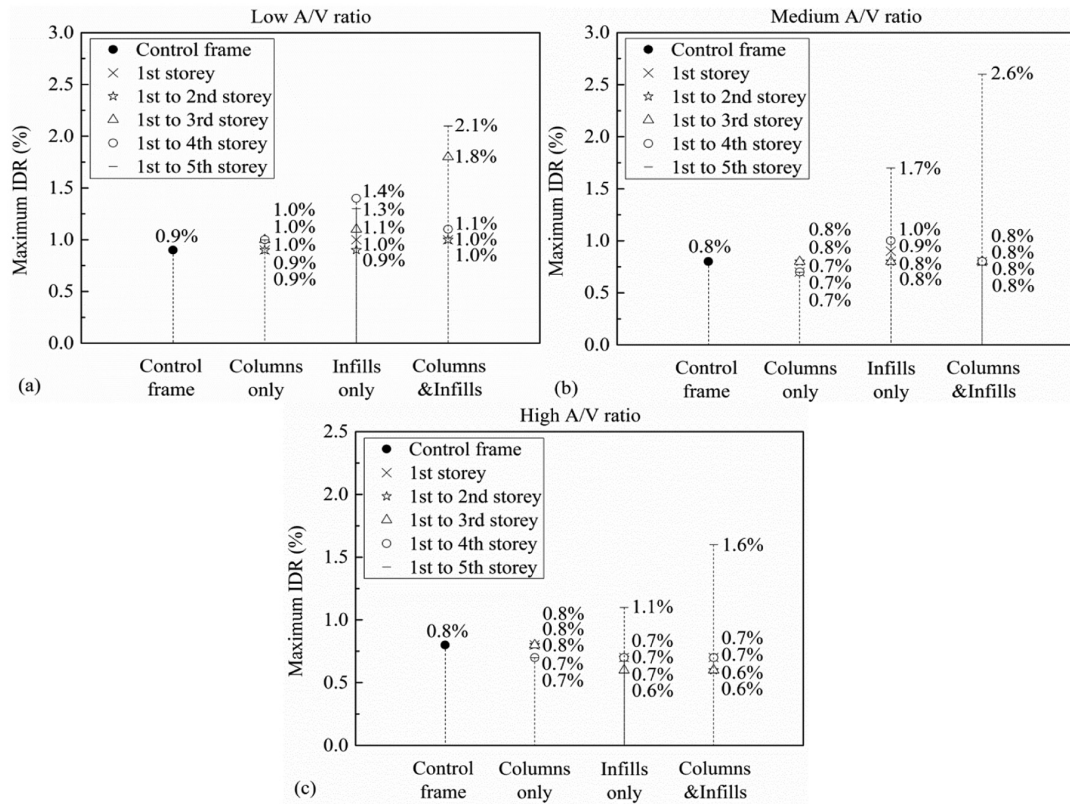
Figure 13. Mean maximum IDR capacity for the control and retrofitted frames: (a) low A/V ratio, (b) medium A/V ratio, and (c) high A/V ratio.

Conclusion

The purpose of this study was to analytically investigate the effectiveness of varying CFRP retrofitting schemes in improving the seismic performance of existing substandard RC frames with masonry infills at high risk of collapse due to out-of-plane earthquake excitations. For this purpose, the IDA analysis was conducted for a typical five-story masonry-infilled RC frame before and after retrofit. Based on the analytical results, the following conclusions can be drawn:

1. For existing substandard RC frames, the collapse of masonry infills due to out-of-plane effect had a significantly adverse impact on the seismic performance of the structures. The mean maximum PGA and IDR capacities of the frame under earthquakes with different frequency contents were reduced by 30%–40%. The collapse of infills also resulted in that the plastic hinges were formed only in columns and the whole structure finally developed a soft-story failure mechanism.

2. The earthquake frequency contents had an obvious influence on the maximum PGA capacity of structures. The maximum PGA resisted

by RC frames increased significantly with the increase in A/V ratio of the ground motions. However, the structures' IDR capacity changed little with respect to the change in the earthquake properties (A/V ratio). This confirms the availability and reliability of using the maximum IDR as a damage parameter to indicate the performance of structures.

3. Retrofitting columns only at either some or all stories was not effective in increasing the maximum PGA, IDR, and energy dissipation capacities of the substandard frame (control frame), especially for medium and high A/V ratio earthquakes. It can be attributed to the fact that the structural behavior was controlled by the nonductile infill, and the collapse of infills could not be prevented when only the RC columns were retrofitted. The methods of retrofitting only infills or retrofitting both columns and infills could provide a degree of enhancement for the control frame under low A/V ratio records, and the increase was more profound as the number of retrofitted stories increased, while for medium and high A/V ratio earthquakes, they were found to be efficient only when more than half of the structure height
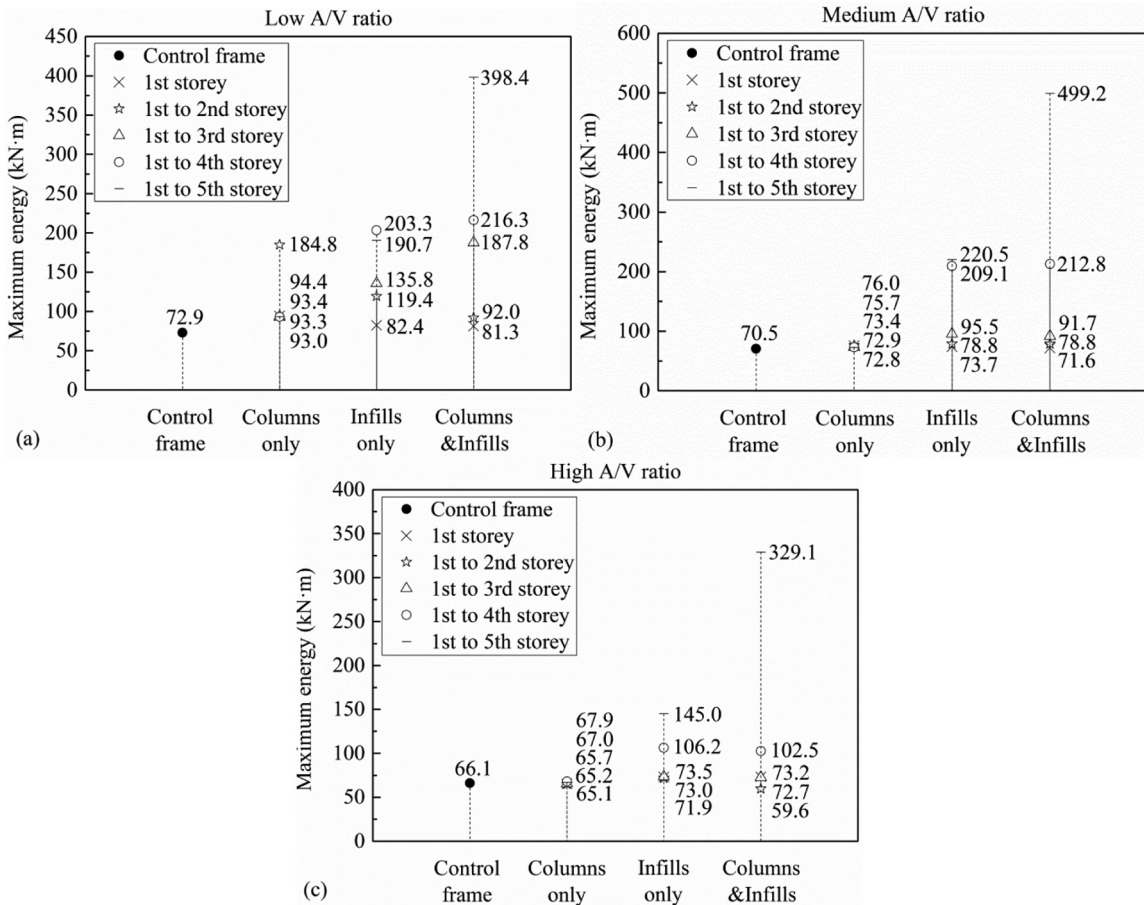
Figure 14. Mean maximum energy dissipated by the control and retrofitted frames: (a) low A/V ratio, (b) medium A/V ratio, and (c) high A/V ratio.

was retrofitted. Compared with other retrofit schemes, the method of retrofitting both columns and infills for the full height of the frame resulted in the most significant increase in the maximum PGA, IDR, and energy dissipation capacities.

4. The results in this study also indicated that the improper selection of a retrofitting scheme was likely to result in the change of the soft-story location, which would cause unexpected damage to structures. By contrast, the maximum IDR capacity of existing substandard RC frame was able to meet the code requirements when an effective retrofitting scheme using CFRP was adopted.

It is important to clarify that the conclusions of this study can be generalized to low-rise RC frame structures. However, the effectiveness of the retrofit schemes on medium- and high-rise structures is expected to be different.

Declaration of Conflicting Interests

Funding

References

Akin E, Ozcebe G, Canbay E, et al. (2014) Numerical study on CFRP strengthening of reinforced concrete frames with masonry infill walls. *Journal of Composites for Construction* 18(2): 04013034.

Al-Salloum YA and Almusallam TH (2007) Seismic response of interior RC beam-column joints upgraded with FRP sheets. I: experimental study. *Journal of Composites for Construction* 11: 575–589.

Altın S, AnılÖ, Emin Kara M, et al. (2008) An experimental study on strengthening of masonry infilled RC frames using diagonal CFRP strips. *Composites Part B: Engineering* 39: 680–693.

Altın S, AnılÖ, Emin Kara M, et al. (2012) Comparison of seismic performance of RC frames strengthened with four different techniques. *Advances in Structural Engineering* 15(2): 343–358.

Baran M and Tankut T (2011) Retrofit of non-ductile RC frames with precast concrete (PC) wall panels. *Advances in Structural Engineering* 14(6): 1149–1166.

Bennett RM, Flanagan RD, Adham S, et al. (1996) *Evaluation and Analysis of the Performance of Masonary Infills during the Northridge Earthquake* (Final report for submission to the National Science Foundation, grant no. CMS-9416262, February, USA). Arlington, VA: National Science Foundation.

Bikce M (2011) How to reduce short column effects in buildings with reinforced concrete infill walls on basement floors. *Structural Engineering and Mechanics* 38: 249–259.

Binici B, Ozcebe G and Ozcelik R (2007) Analysis and design of FRP composites for seismic retrofit of infill walls in reinforced concrete frames. *Composites Part B: Engineering* 38: 575–583.

Braga F, Manfredi V, Masi A, et al. (2011) Performance of non-structural elements in RC buildings during the L'Aquila, 2009 earthquake. *Bulletin of Earthquake Engineering* 9: 307–324.

Cagatay IH, Beklen C and Mosalam KM (2010) Investigation of short column effect of RC buildings: failure and prevention. *Computers and Concrete* 7: 523–532.

Carpinteri A, Cornetti P, Lacidogna G, et al. (2009) Towards a unified approach for the analysis of failure modes in FRP-retrofitted concrete beams. *Advances in Structural Engineering* 12(5): 715–729.

Correnza JC, Hutchinson GL and Chandler AM (1994) Effect of transverse load-resisting elements on inelastic earthquake response of eccentric-plan buildings. *Earthquake Engineering & Structural Dynamics* 23: 75–89.

Dandapat R, Deb A and Bhattacharyya SK (2011) Failure modes for FRP wrapped cylindrical concrete columns. *Journal of Reinforced Plastics and Composites* 30: 561–579.

De Stefano M, Faella G and Ramasco R (1998) Inelastic seismic response of one-way plan-asymmetric systems under bi-directional ground motions. *Earthquake Engineering & Structural Dynamics* 27: 363–376.

Deng J, Liu A, Ma ZJ, et al. (2015) Interfacial behavior of RC beams strengthened with FRP under fatigue loading. *Advances in Structural Engineering* 18(2): 283–294.

Dolsek M and Fajfar P (2001) Soft storey effects in uniformly infilled reinforced concrete frames. *Journal of Earthquake Engineering* 5: 1–12.

El-Sokkary H and Galal K (2009) Analytical investigation of the seismic performance of RC frames rehabilitated using different rehabilitation techniques. *Engineering Structures* 31: 1955–1966.

Erdem I and Akyuz U (2010) Analytical investigation of lateral strength of masonry infilled RC frames retrofitted with CFRP. *Journal of Performance of Constructed Facilities* 24: 302–310.

Federal Emergency Management Agency (FEMA) (2000a) *Prestandard and commentary for the seismic rehabilitation of buildings.* Report no. FEMA-356, November. Washington, DC: FEMA.

Federal Emergency Management Agency (FEMA) (2000b) *Recommended seismic design criteria for new steel moment-frame buildings.* Report no. FEMA-350, June. Washington, DC: FEMA.

Galal K and El-Sokkary H (2008) Analytical evaluation of seismic performance of RC frames rehabilitated using FRP for increased ductility of members. *Journal of Performance of Constructed Facilities* 22: 276–288.

Garcia R, Hajirasouliha I and Pilakoutas K (2010) Seismic behaviour of deficient RC frames strengthened with CFRP composites. *Engineering Structures* 32: 3075–3085.

Guo ZH (1999) *Principle of Reinforced Concrete.* 1st ed. Beijing, China: Tsinghua University Press (in Chinese).

Hashemi SA and Mosalam KM (2006) Shake-table experiment on reinforced concrete structure containing masonry infill wall. *Earthquake Engineering & Structural Dynamics* 35: 1827–1852.

Hashemi SA and Mosalam KM (2008) *Modeling of unreinforced masonry infill walls considering in-plane and out-of-plane interaction.* Pacific Earthquake Engineering Research Center (PEER) 2008/102. Available at: https://peer.berkeley.edu/publications/peer_reports/reports_2008/web_PEER8102_Kadysiewski_Mosalam_R.pdf

Kakaletsis D (2011) Comparison of CFRP and alternative seismic retrofitting techniques for bare and infilled RC frames. *Journal of Composites for Construction* 15: 565–577.

Ma G, Li H and Wang J (2013) Experimental study of the seismic behavior of an earthquake-damaged reinforced concrete frame structure retrofitted with basalt fiber-reinforced polymer. *Journal of Composites for Construction* 17(6): 04013002.

Ministry of Construction of the People's Republic of China (2002) *GB50010: Code for Design of Concrete Structures.* Beijing, China: China Architecture and Building Press (in Chinese).

Ministry of Construction of the People's Republic of China (2010) *GB50010: Code for Design of Concrete Structures.* Beijing, China: China Architecture and Building Press (in Chinese).

Mukherjee A and Jain KK (2013) A semi-analytical model of cyclic behavior of reinforced concrete joints rehabilitated with FRP. *Advances in Structural Engineering* 16(12): 2019–2034.

Ozcelik R, Akpınar U and Binici B (2011) Seismic retrofit of deficient RC structures with internal steel frames. *Advances in Structural Engineering* 14(6): 1205–1222.

Ozkaynak H, Yuksel E, Buyukozturk O, et al. (2011) Quasi-static and pseudo-dynamic testing of infilled RC frames retrofitted with CFRP material. *Composites Part B: Engineering* 42: 238–263.

PERFORM-3D User Guide (2011) *Nonlinear Analysis and Performance Assessment for 3D Structures* (version 5). Berkeley, CA: Computers and Structures, Inc.

Smith ST and Teng JG (2002) FRP-strengthened RC beams. I: review of debonding strength models. *Engineering Structures* 24: 385–395.

Tso WK, Zhu TJ and Heidebrecht AC (1992) Engineering implication of ground motion A/V ratio. *Soil Dynamics and Earthquake Engineering* 11(3): 133–144.

Uva G, Raffaele D, Porco F, et al. (2012) On the role of equivalent strut models in the seismic assessment of infilled RC buildings. *Engineering Structures* 42(12): 83–94.

Vamvatsikos D and Cornell CA (2002) Incremental dynamic analysis. *Earthquake Engineering & Structural Dynamics* 31: 491–514.

Verderame GM, De Luca F, Ricci P, et al. (2011) Preliminary analysis of a soft-storey mechanism after the 2009 L'Aquila earthquake. *Earthquake Engineering & Structural Dynamics* 40: 925–944.

Wang DY, Wang ZY, Yu T, et al. (2016) Shake table tests of large-scale substandard RC frames retrofitted with CFRP wraps before earthquakes. *Journal of Composites for Construction* 21(1): 04016062.

Wang WW, Dai JG and Harries KA (2013) Intermediate crack-induced debonding in RC beams externally strengthened with prestressed FRP laminates. *Journal of Reinforced Plastics and Composites* 32: 1842–1857.

Wang ZY, Wang DY, Smith ST, et al. (2012a) CFRP-confined square RC columns. I: experimental investigation. *Journal of Composites for Construction* 16: 150–160.

Wang ZY, Wang DY, Smith ST, et al. (2012b) CFRP-confined square RC columns. II: cyclic axial compression stress-strain model. *Journal of Composites for Construction* 16: 161–170.

Wang ZY, Wang DY, Smith ST, et al. (2012c) Experimental testing and analytical modeling of CFRP-confined large circular RC columns subjected to cyclic axial compression. *Engineering Structures* 40: 64–74.

Yuksel E, Ozkaynak H, Buyukozturk O, et al. (2010) Performance of alternative CFRP retrofitting schemes used in infilled RC frames. *Construction and Building Materials* 24: 596–609.

Zou XK, Teng JG, De Lorenzis L, et al. (2007) Optimal performance-based design of FRP jackets for seismic retrofit of reinforced concrete frames. *Composites Part B: Engineering* 38: 584–597.